
THEORETICAL ANALYSIS OF CONCENTRATION POLARIZATION EFFECT ON VOC REMOVAL BY PERVAPORATION

¹S.X. Liu, ²L.M. Vane, and ¹M. Peng

¹*Department of Food Science, Rutgers University, New Brunswick, New Jersey 08901-8520; Phone: (732) 932-9611 X240; Fax: (732) 932-6776; Email: liu@aesop.rutgers.edu.*

²*Clean Process and Product Division, National Risk Management Research Laboratory, U.S. Environmental Protection Agency, 26 W. Martin L. King Dr., Cincinnati, Ohio 45268; Phone: (513) 569-7799; Email: vane.leland@epa.gov.*

ABSTRACT

Pervaporation is an innovative membrane-based separation technology for volatile organic compound (VOC) removal from contaminated groundwater. Concentration polarization is a process phenomenon occurring in pervaporation and several other membrane-based separation technologies. Concentration polarization, defined as concentration gradient of permeating solute between the bulk and the region near the membrane surface, becomes a limiting factor in pervaporation separations using high-performance membrane materials in VOC removal operations. Thus, the ability to predict the impact of concentration polarization upon process performance is highly desirable in process design and optimization. A mathematical model was developed to illustrate the interplay between concentration polarization and process performance in pervaporation operation of VOC removal in a membrane channel with rectangular cross section. By incorporating pervaporative mass transfer, laminar hydrodynamics, and boundary-layer theory, the model was built to allow theoretical analysis of the sensitivity of flow velocity, feed concentration, and concentration polarization index (CPI) upon the transmembrane flux and longitudinal mass flow.

Key words: pervaporation, concentration polarization, VOC removal, boundary-layer mass transfer

INTRODUCTION

Volatile organic compound (VOC) removal from contaminated groundwater by pervaporation is a membrane-based environmental technology that achieves separation of liquid mixtures with minimal mechanical and thermal energy inputs. The overall process is a combination of evaporation and membrane permeation occurring continuously and simultaneously. Acting as a semi-permeable barrier, a non-porous perm-selective membrane is able, under proper operating conditions, to remove dissolved VOCs from water (Jiang et al., 1997a; Vane et al., 1999; Abou-Nemeh et al., 1999; George et al., 2000; Uragami et al., 2001; Vane and Alvarez, 2002; Peng and Liu, 2003b), dehydrate alcohols (Shieh and Huang, 1998; Lee et al., 2000; Jiratananon et al., 2002; Hilmioglu and Tulbentci, 2003; Aiouache and Goto, 2003), recover food aroma compounds (Karlsson and Trägårdh, 1996; Alvarez et al., 2000; Shepherd et al., 2002; Peng and Liu, 2003a), and separate mixtures of components with close boiling points or azeotropes that are difficult to separate by distillation or other conventional separation technologies (Böddiker et al., 1990a; Böddiker et al., 1990b; Kusakabe et al., 1998; Matsui and Paul, 2003). For a general review of VOC removal by pervaporation, the reader is referred to the paper written by the authors (Peng

et al., 2003). Pervaporation is a contraction of words describing the two major operations involved in the separation process, namely, permeation and evaporation, and is defined as a separation process in which a liquid feed mixture is separated by means of partial diffusion-vaporization through a non-porous polymeric membrane. Pervaporation is usually carried out by placing a liquid stream containing two or more species in contact with one side of the membrane, while a vacuum or sweeping gas is applied to the other side. The species, with various affinities to the membrane sorb into the membrane, permeate through it and evaporate into the vapor phase. The vapor is then condensed. The membrane can be considered as a dense homogenous medium in which diffusion of species takes place in the free volume present between the macromolecular chains of the membrane material. Thus, pervaporation represents a new type of unit operation with the potential to replace a number of conventional separation processes for some separation tasks.

The decision as to whether to use a pervaporation process for a particular task or not must be weighed against competing conventional separation technologies. In evaluating advantages and disadvantages for a pre-set objective, or the performance of an existing pervaporation operation, one would benefit from a descriptive reliable physical model that permits sufficiently accurate estimation of the technical and economic feasibility and potentials or shortcomings. As a result, better membranes and/or module designs will be developed and adopted for environmental separations. As the price and performance of commercial membranes for VOC removal look increasingly attractive to environmental scientists and engineers these days, more research attention has been paid to process and module design. In particular, many researchers in the pervaporation field have focused on modeling mass transfer in the boundary layer on the upper stream side of the membrane unit, since results of these efforts will have significant impact on both performance and economics of a commercial-scale pervaporation unit for environmental cleanup, and ultimately acceptance of this technology for VOC removal. One of the most important aspects in developing mass transfer modeling for pervaporation processes is concentration polarization prediction and assessment. Concentration polarization is a membrane process phenomenon that adversely affects the performance of pervaporation treatment of groundwater contaminated with VOCs. It mainly occurs on the upstream side of the membrane and manifests as a steep discrepancy of

concentrations between the solute concentration in the bulk (which can be measured) and that in the thin layer adjacent to the membrane surface (which is not measurable). Obviously, concentration polarization reduces the available driving force across the membrane, since the VOC mass transfer rate is controlled by the difference between chemical potentials (approximated by concentrations) in the boundary layers at both sides of the membrane. Thus, there is a market for mass transfer models that are able to predict the impact of concentration polarization on process performance under certain operating conditions for a particular membrane module configuration. Once the sources of problems associated with pervaporation operations are identified and quantified, the plant operator can then muster necessary technical resources to implement remedies to combat process problems caused by concentration polarization.

CONCENTRATION POLARIZATION

Mass transfer in a pervaporation process can be properly described as, based upon basic transport functions, a solution-diffusion mechanism (Binning et al., 1961) that delineates the mass transfer with the following steps:

1. Diffusion through the liquid boundary layer next to the feed side of the membrane.
2. Selective partitioning of molecules of components into the membrane.
3. Selective transport (diffusion) through the membrane matrix.
4. Desorption into the vapor phase on the permeate side.
5. Diffusion away from the membrane and into the vapor boundary layer on the permeate side of the membrane.

Often each step can be modeled with different approaches and fundamental assumptions; however, as with all mass transfer operations, the slowest step in this sequence will limit the overall rate of mass transfer and will be the center of research focus. The slowest step is determined by membrane characteristics, fluid flow regimes on each side of the membrane, properties of the component being separated, and properties of the phases that are involved. Partitioning and desorption steps (steps 2 and 4) are generally not considered to be rate-limiting. Indeed, it is usually assumed that an equilibrium condition prevails at the interface between the membrane and the fluid phases; therefore, one or more of steps 1, 3, and 5 may control the rate of mass transfer. Naturally, these steps are conveniently expressed

in the form of the resistance-in-series analogy as in the case of an electrical circuit, which can be expressed with mathematical symbols as:

$$\frac{1}{k^{ov}} = \frac{1}{k^{bl}} + \frac{1}{k^m} + \frac{1}{k^v} \quad (1)$$

The k s appearing in the equation are mass transfer coefficients, and their reciprocals represent the mass transfer resistance at each step. For many pervaporation processes involving dilute solutions, the mass transfer resistance in the vapor boundary layer tends to be small enough to be ignored since the concentration of VOC is very low. k^m is strongly determined by polymer properties, thickness of the membrane, and chemical and physical properties of the components in the liquid. Although the membrane is at the heart of a pervaporation separation, many membrane materials currently available for VOC removal operations are composite polymers with ultra-thin active layers and impose very little transfer resistance to permeating species. As a result, VOC mass transfer resistance in many well-studied systems, to a large extent, is limited by mass transport of VOC molecules in the feed-side liquid boundary layer. This rate-limiting effect is often manifested as concentration polarization. Existence of concentration polarization in a pervaporation process affects process performance (permeation flux and selectivity) adversely.

Concentration polarization has been receiving a growing amount of attention in the pervaporation field. Michael (1995) pointed out that in very dilute, sparingly soluble organic-water systems, liquid boundary layer resistance might be the dominating factor in overall consideration of pervaporation mass transfer. His observation was corroborated by a number of investigators (Psaume et al., 1986; Côté and Lipski, 1988; Wijmans et al., 1996; Jiang et al., 1997a; Bhattacharya and Hwang, 1997; Rautenbach and Hommerich, 1998; Higuchi et al., 2002).

In many studies of concentration polarization, Sherwood correlations were often invoked to correlate the upstream mass transfer resistance with a thin layer of stagnant film that is usually assumed to exist next to the membrane (Peng et al., 2003). Sherwood correlations are based upon parallels with earlier studies of fluid mechanics and heat transfer of a simple physical system that may not always give out accurate results that can be verified with experimental data. This imperfection, however, does not preclude Sherwood correlations being a useful customary tool used for interpreting experimental data.

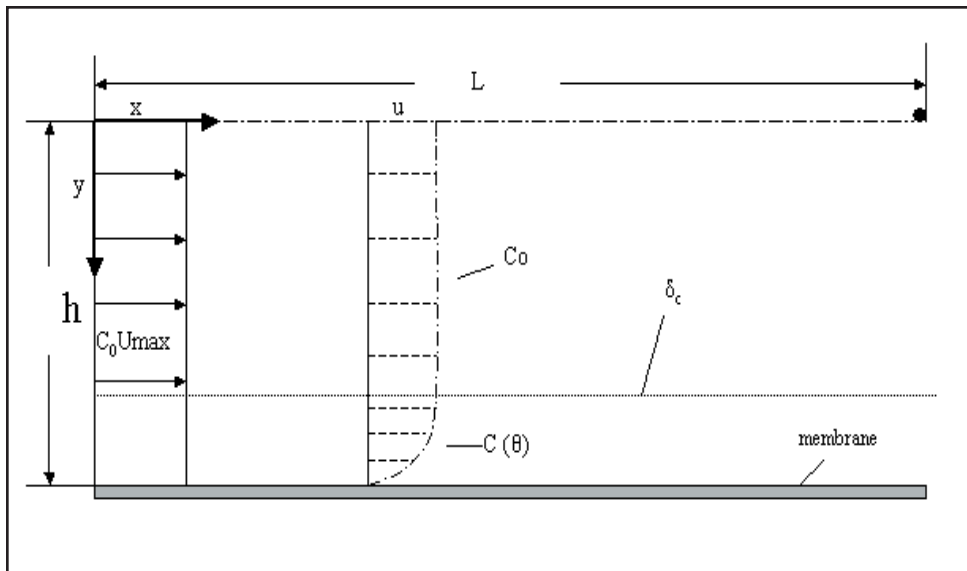


Figure 1. Flow and concentration boundary layers in a membrane channel (only the bottom half of flow channel is shown).

This is because Sherwood correlations tend to be straightforward and do not involve complex numerical computational schemes and enormous amounts of computing power, unlike the approach of establishing and solving Navier-Stokes and mass transfer equations (which undoubtedly give out more precise results). By incorporating a form of the Sherwood correlation prescribed to a particular membrane geometrical configuration into the overall mass transport model, one can analyze with relative ease the effects of concentration polarization and other process parameters such as feed concentration and feed flow rate on pervaporation process performance. Therefore, the objective of this paper was to develop a pervaporation mass transfer model that adequately described the mass transfer in a pervaporation membrane channel without being entangled in mathematical conundrums.

MODEL DEVELOPMENT

A pervaporation membrane channel with rectangular cross section was considered. One dimension of the cross section, corresponding to the distance, $2h$, between the non-porous membrane walls, was taken to be much smaller than the width of the flow channel. This condition enabled the problem to be treated as a case of two-dimensional flow. Both channel walls were considered as having equal permeability. The equations had to be written over the elementary control volume as shown in Figure 1. Further mathematical treatment was based upon the following underlying assumptions:

1. The flow was assumed to be incompressible, continuous, isothermal laminar, and steady state.
2. The concentration of contaminant (VOC) on the vapor side was negligible (Jiang et al., 1997a; Peng and Liu, 2003a, 2003b).
3. There was no mass transfer across the symmetry plane that delineates the mid-points between the walls and sides of the gap.
4. The distance between inner membrane surface and axial line was assumed to be equal to the hydrodynamic boundary layer: $\delta = h$.
5. The flow is assumed fully developed so that the velocity boundary-layer thickness, δ , is constant along the membrane surface.
6. Diffusion of the solute in the horizontal direction of the channel, x , is negligible while convection of the solute in y direction (perpendicular to the membrane walls) is neglected.
7. The flow entered the channel with a uniform velocity of U_{\max} and upon entering the flow is instantaneously fully developed.

The modeling effort described here comprises development of a correlation between longitudinal mass flow rates of permeating VOC and parameters of concentration and velocity profiles in the boundary layer in the slit formed by the membrane walls. Since the flow is symmetrical about a plane midway between the walls, the modeling solution will be carried out over half the channel, i.e., from the mid-plane to one wall. The general equation for the longitudinal mass flow rate of a model VOC, M_{long} , can be represented mathematically as:

$$M_{\text{long}} = \iint_A u(y) \cdot c(y) dA \quad (2)$$

where feed velocity parallel to membrane is designated by y -component of velocity in the horizontal direction, $u(y)$, of which there exists a gradient in the direction that is perpendicular to the membrane walls; $c(y)$ is the concentration field in the same direction as the velocity field; y is the coordinate in Figure 1; and $dA = W dy$ is the control cross section normal to the membrane walls where W is the width of the gap. In order for the analytical solution to be developed, the hydrodynamic and concentration fields

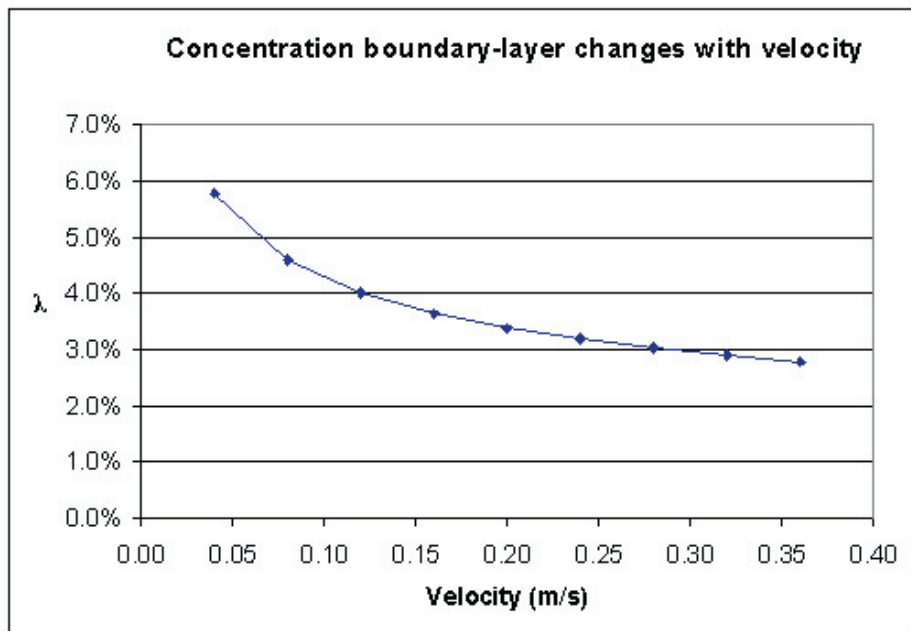


Figure 2. Influence of feed velocity on dimensionless concentration boundary-layer thickness.

have to be approximated and incorporated into Equation (2). We started out by introducing dimensionless coordinates:

$$\eta = \frac{h-y}{h} \quad (3)$$

$$\theta = \frac{\eta}{\lambda} \quad (4)$$

The coordinate η varies from 0 to 1 and its unit of scale in the coordinate is equal to the thickness of current hydrodynamic layer, δ . The coordinate η is introduced to describe the hydrodynamic field; therefore, the velocity profile is expressed in terms of the η coordinate. The other dimensionless coordinate θ is launched to depict the profiles within the diffusion layer (concentration) between $y=h$ to $y=h-\delta_c$, where δ_c is the thickness of the current diffusion layer. The unit of scale in the θ coordinate is the concentration boundary layer thickness, λ in η coordinate. λ represents the relative thickness of boundary layer and is equal to δ_c / h .

In order to describe the hydrodynamic boundary layer, a mathematical function whose curve corresponds to the shape of the physical profile of velocity distribution in the boundary layer is needed. Various approximations of velocity profiles have been compared in boundary-layer studies for

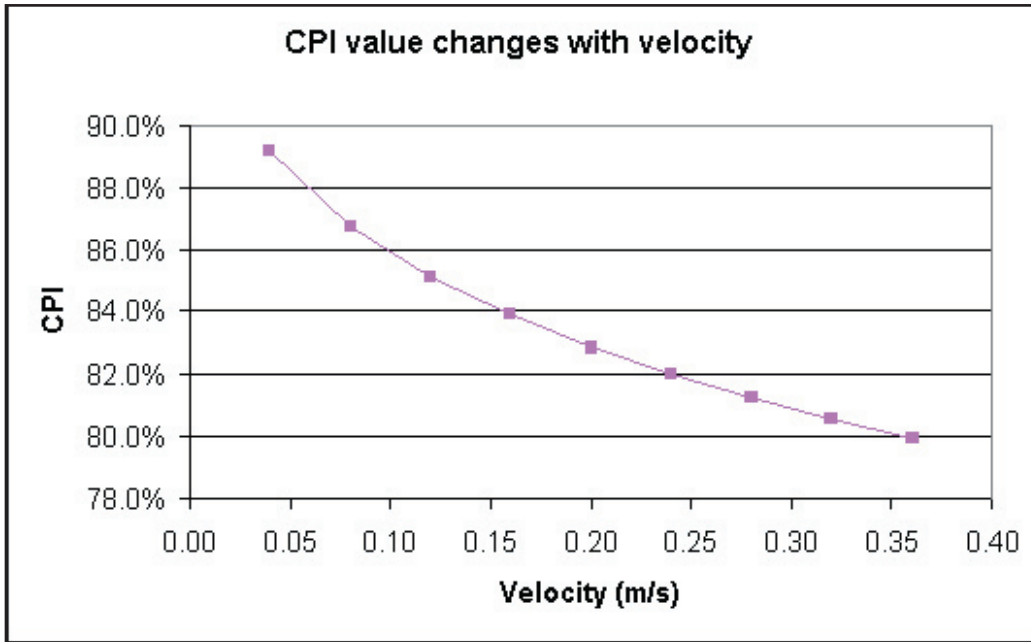


Figure 3. Dependence of CPI on velocity.

different flow-solid interactions (Schlichting, 1979). For a laminar flow in a parallel slit, the velocity in the control volume can be expressed as (Bird et al., 2001):

$$u(y) = 2U_{\max} \left(1 - \frac{y^2}{h^2}\right) \quad (5)$$

where $2U_{\max}$ is the velocity at the mid-plane parallel to the membrane walls, and h is the half distance between the walls. Please note, we have assumed that the mass transfer across the membrane is small; therefore, the parabolic velocity profile between the walls is unaltered in a pervaporation operation. If the mass transfer rate is sufficiently high, a perturbation function has to be incorporated into the hydrodynamic consideration to obtain the profile (Berman, 1953). Using the dimensionless variables to re-arrange Equation (5) yields:

$$u(\eta) = 2U_{\max} (2\eta - \eta^2) \quad (6)$$

$$u(\theta) = 2U_{\max} (2\theta\lambda - \theta^2\lambda^2) \quad (7)$$

The new boundary conditions are $u(\theta=0) = 0$ at the membrane surface; and $u(\theta=1) = u(\eta=\lambda)$ at the border of the diffusion layer (the edge of the concentration profile). Like the hydrodynamic field, the concentration field also needs to be estimated with a reasonably uncomplicated mathematical function

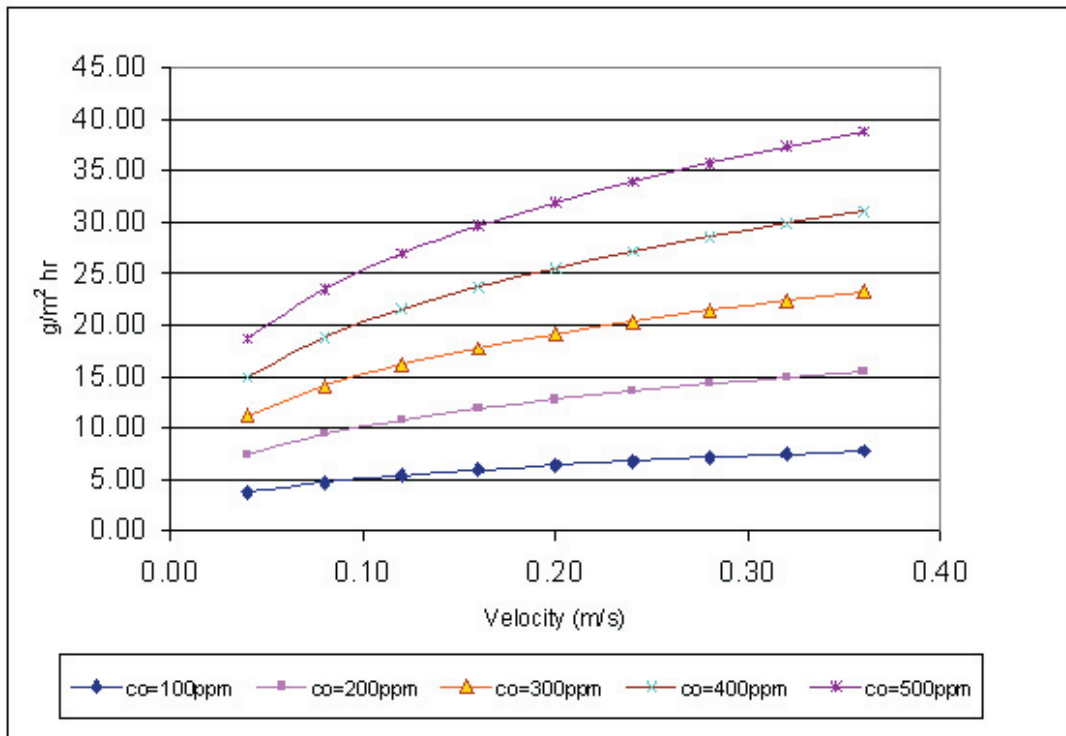


Figure 4. Effect of feed velocity on PV transmembrane VOC flux.

or expression. It is customary to express the concentration distribution in a parallel slit free from external forces in the diffusion layer in the following way (Bird et al., 2001; Cussler, 1997):

$$\frac{c(\theta) - c_0}{c_m - c_0} = 1 - (2\theta - \theta^2) = (1 - \theta)^2 \quad (8)$$

where c_m is the concentration of dissolved VOC at the membrane surface. Equation (8) may be stated in terms of the concentration polarization index (CPI):

$$c(\theta) = c_0 [1 - CPI(1 - \theta)^2]$$

where:

$$CPI = \frac{c_0 - c_m}{c_0} \quad (9)$$

In steady state operation, the solute flux through the membrane and from the boundary layer to the membrane are the same: $k^m * c_0 (1 - CPI) = D^*(c_0 - c_m) / \delta_c$. Using this equation and the definitions of λ and CPI, the relationship between λ and CPI can be established as:

$$CPI = \frac{1}{1 + D / (k^m * h * \lambda)} \quad (10)$$

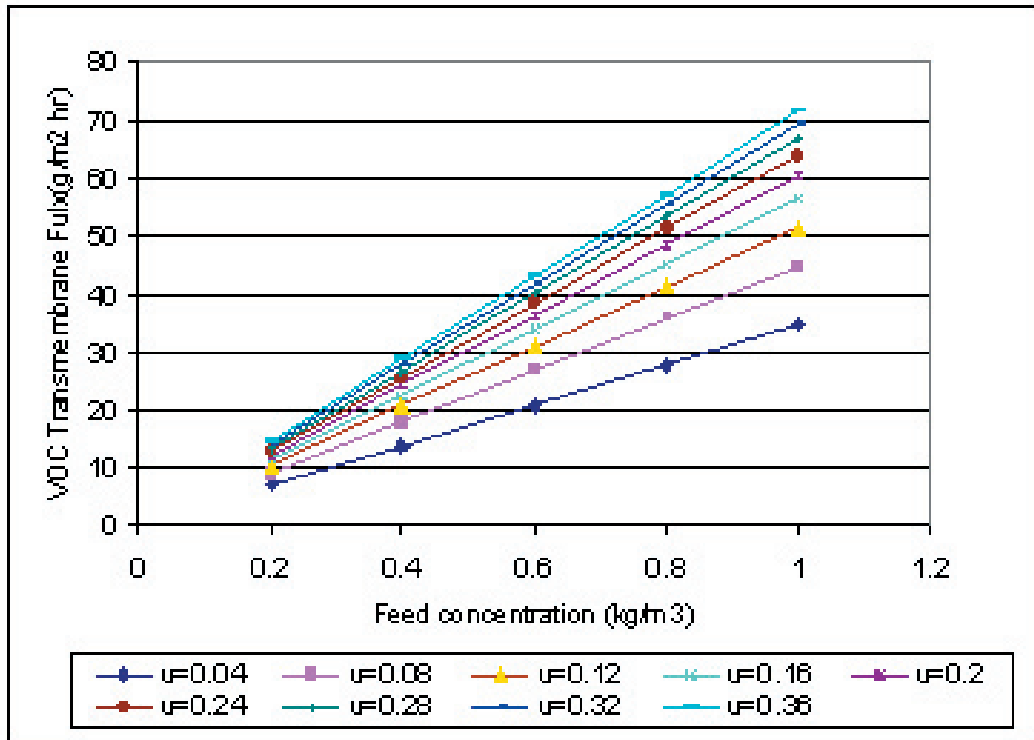


Figure 5. Trans-membrane VOC flux as a function of VOC feed concentration.

D is the diffusion coefficient of solute in solution. The longitudinal mass flow rate expressed in Equation (2) can be simplified by taking into account the assumptions and geometry of the control volume, which gives:

$$M_{long} = \int_{y=0}^{y=h} u(y)c(y)Wdy \quad (11)$$

where W is the width of the control volume. Equation (11) can be further simplified by decomposing it into two components. One component accounts for the contribution to the mass flow rate in the diffusion layer, and the other represents the part of mass flow rate outside the diffusion layer:

$$M_{long} = \int_{y=h-\delta_c}^{y=h} u(y)c(y)Wdy + \int_{y=0}^{y=h-\delta_c} u(y)c(y)Wdy \quad (12)$$

The first term on the right-hand side of Equation (12) can be transformed by substituting Equations (7) and (9) into u(y) and c(y) variables, and the resulting expression reflects the mass flow of VOC within the diffusion layer in the coordinate θ . The mathematical treatment of this term produces:

$$M_{long}^{diff} = 2U_{max}c_0Wh\left[\left(1 - \frac{CPI}{6}\right)\lambda^2 - \left(\frac{1}{3} - \frac{CPI}{30}\right)\lambda^3\right] \quad (13)$$

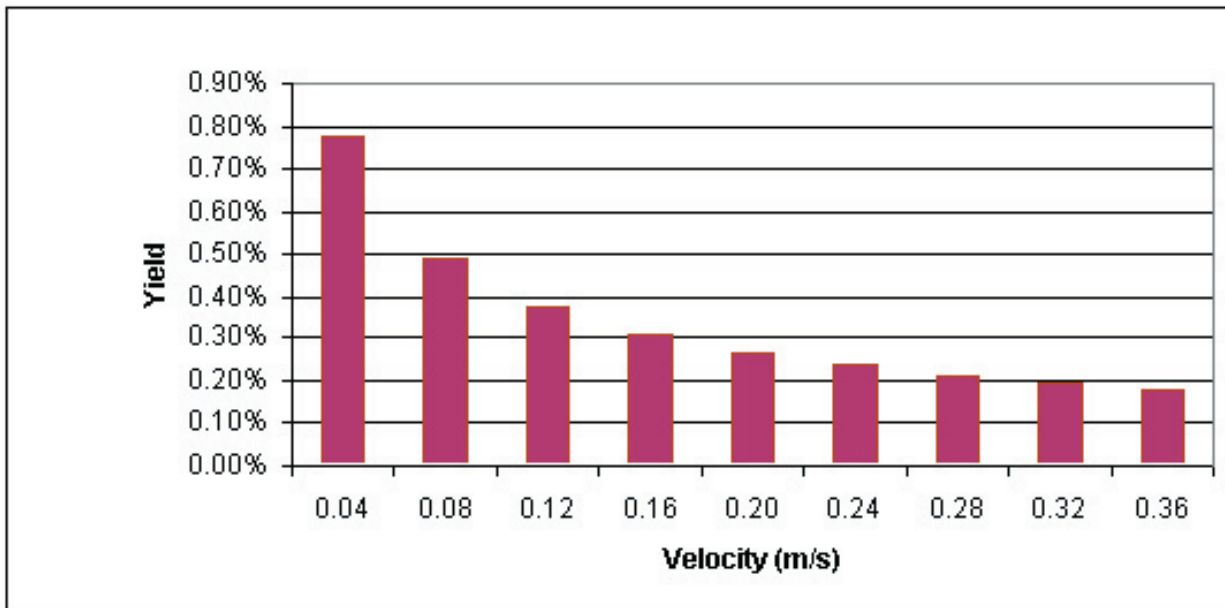


Figure 6. PV operation yield as a function of velocity.

The second term on the right side of Equation (12) is the mass flow in the region between the border of the diffusion-boundary layer and the mid-plane of the slit, M_{long}^b . It can also be integrated using the dimensionless expression in Equation (7):

$$M_{long}^b = 2U_{max}c_0Wh\left[\frac{\lambda^3}{3} - \lambda^2 + \frac{2}{3}\right] \quad (14)$$

The longitudinal mass flow rate at inlet becomes:

$$M_{long} = 2U_{max}c_0Wh(A + B) \quad (15)$$

where A is

$$A = \left[\left(1 - \frac{CPI}{6}\right)\lambda^2 - \left(\frac{1}{3} - \frac{CPI}{30}\right)\lambda^3 \right] \quad (16)$$

and B is

$$B = \left[\frac{\lambda^3}{3} - \lambda^2 + \frac{2}{3} \right] \quad (17)$$

After passing through the membrane module, the concentration of VOC in solution will have decreased due to the permeation of solute. The reduced mass flow rate at the outlet can be expressed by an equation

similar to equation (15), with the decreased concentration replacing c_0 . The difference of longitude mass flow rate can be expressed in differential form and can be correlated to the overall mass transfer coefficient as:

$$2U_{\max}Wh(A+B)(-dc) = W \cdot k^{bl} \cdot (c - c_m) \cdot dx \quad (18)$$

x is the length from the inlet; k^{bl} is the mass transfer coefficient in the concentration boundary layer; and c is the VOC concentration in bulk solution. By separating variables and utilizing boundary conditions of $c=c_0$ at $x=0$ and $c=c'$ at $x=L$, the concentration of outgoing solution can be obtained as:

$$\ln c' = \ln c_0 - \frac{k^{bl}LCPI}{2U_{\max}h(A+B)} \quad (19)$$

The value of k^{bl} usually could not be obtained before experimental data was available. The conventional approach has been using a semi-empirical correlation equation for membrane channel configuration (Mulder, 1991):

$$k^{bl} = 1.85 \left(\frac{U_{\max} D^2}{d_n L} \right)^{1/3} \quad (20)$$

where D is the diffusivity of solute in the solution, d_n the hydraulic diameter of the liquid flow path, L the length of module, and U_{\max} the average feed solution velocity. This correlation was originally used in

Table 1. Semi-empirical correlations for mass transfer coefficient in concentration boundary layer.

System	k_{bl}
Hollow fiber	$Sh = 0.026 Re^{0.8} Sc^{1/3}$ [1]
Spiral wound, $Re < 1,000$	$Sh = 0.065 Re^{0.875} Sc^{1/4}$ [1]
Transversal, $Re < 1,000$	$Sh = 0.90 Re^{0.4} Sc^{1/3}$ [1]
Circular cell with two parallel plates	$Sh = 0.30 Re^{1/2} Sc^{1/3}$ [1]
Laminar, tubular	$Sh = 1.62 Re_r^{1/3} Sc^{1/3} (2R/L)^{1/3}$ [1]
Rectangular membrane channel	$Sh = 1.82 Re_h^{1/3} Sc^{1/3}$ [2]
Cell with radial flow $100 < Re_r < 635$	$k = 552.2 (Re_r)^{1/3} Sc^{1/3}$ [3]
Slit membrane flow channel $20 < Re < 500$	$k = 0.145 Re^{1/2}$ [4]
Radial flow between parallel plates $70 < Re < 5,000$	$Sh = 1.80 Re^{0.47} Sc^{1/3}$ [5]
Conical cell with radial flow $100 < Re_r < 874$	$Sh(r) = 0.81 [Re(r)]^{1/2} Sc^{1/3}$ [6]

Where $Sh = kl/D$, $Re = \rho u \mu$, $Sc = \mu/D\rho$, and $R =$ radius.

Note: in a Sherwood correlation, l represents characteristic length of module, such as radius or diameter for circular tube or hydraulic diameter for non-circular channels. Sources: [1] Lipski and Cote (1990), [2] Mulder (1991), [3] Dotremont et al. (1994), [4] Jiang et al. (1997b), [5] Bandini et al. (1997), and [6] Urtiaga et al. (1999).

heat transfer research and the analogy was assumed to exist between these heat transfer and mass transfer phenomena. As the trans-membrane flow rate in pervaporation is usually small, the contribution from convection to permeation could be neglected. The diffusion is thus responsible for the mass transfer coefficient:

$$k^{bl} = D / \delta_c \quad (21)$$

Equation (21) can be easily re-arranged to:

$$\delta_c = (D / k^{bl}) \quad (22)$$

The concentration boundary-layer thickness under steady operation can also be correlated to the bulk velocity as:

$$\delta_c = (1/1.85) \cdot \left(\frac{d_n LD}{U_{\max}} \right)^{1/3} \quad (23)$$

This will make it possible to calculate the relative thickness of the concentration boundary layer. The yield of the pervaporation operation, which was defined as the ratio of the decrease in solute concentration to the original solute concentration in the feed solution, can be expressed as:

$$Y = 1 - e^{\left(-\frac{k^{bl} LCPI}{2(A+B)hU_{\max}} \right)} \quad (24)$$

The trans-membrane flux is thus expressed as:

$$\frac{M_{trans}}{L \cdot W} = 2U_{\max} c_0 Y h(A + B) / L \quad (25)$$

Therefore, at steady state the transmembrane flux is correlated to the bulk velocity in the module, the difference between the longitudinal flux at the inlet and outlet ($x = 0$ and $x=L$) of the module, and concentration polarization characteristics. Thus, by changing those operating parameters that influence the extent of concentration polarization the overall mass transfer coefficient will be changed accordingly, which will lead to alteration of the transmembrane flux.

SIMULATION AND RESULTS DISCUSSION

In this section, simulation results are given for the separation of VOC from dilute solutions. The pervaporation configuration was composed of polydimethylsiloxane (PDMS) membranes in a slit configuration. The concentration was assumed to be below 500 ppm; the maximum velocity of the feed stream

was restricted to the range of 0.1 to 0.4 m/s (within laminar flow regime); and the length, width, and height of the slit were 0.8m, 0.5m, and 0.01m, respectively. The diffusivity of VOC used in the calculations was $3 \times 10^{-9} \text{m}^2/\text{s}$, based on the Wilke-Chang equation (Cussler, 1997). Calculated results are shown in Figures 2 to 6.

As is shown in Figures 2 and 3, with the increase of feed velocity, the CPI decreases, thus indicating that concentration polarization will be less severe. The transmembrane flux calculated from the difference of outgoing longitudinal mass flow rate from total mass flow rate upon entering the membrane channel is shown in Figure 4. The transmembrane mass flux increases with the increase of feed velocity. The effect of increasing feed concentration on transmembrane flux is also visualized in Figure 5. It can be seen that a linear relationship exists between feed concentration and permeation flux.

As is evident in Figures 2 and 3, feed velocity had great influence on both relative thickness of the boundary layer (λ) and the concentration polarization index (CPI). When the feed velocity was at the low end, the increase in velocity brought significant decreases in λ and CPI, indicating that concentration polarization was severe when flow velocity was low. However, when the flow velocity reached the high end, the extent of λ and CPI reductions was less considerable. As the flow velocity in a membrane module is constrained by configurations of the membrane and its auxiliary components, this explains partially why concentration polarization is difficult to totally eliminate in PV operations.

Transmembrane flux, calculated from the difference between outgoing longitudinal mass flow rate and total mass flow rate upon entering the membrane channel, is shown in Figure 4. Transmembrane mass flux increases with the increase in feed velocity for all feed concentrations. Percentage increase in transmembrane flux with a certain velocity increase is the same for different concentrations, though at high concentration a higher permeation rate, such as $30 \text{g}/\text{m}^2\text{hr}$, would be obtained. The effect of increasing feed concentration on transmembrane flux is also visualized in Figure 5. The linear regression results indicate that a linear relationship exists between feed concentration and permeation flux.

The relationship between yield and velocity is illustrated in Figure 6. It can be seen that yield decreased exponentially with the increase in bulk velocity, according to Equation (23). This is because at a higher velocity, the concentration boundary-layer thickness is thinner (the concentration at the interface

is lower) and the yield decreases substantially, since the bulk velocity is proportional to the concentration boundary-layer thickness, raised to the power of three.

Equation (20) for k^{bl} was used to derive Equations (24) and (25). This correlation (Mulder, 1991) by no means is the only one available for describing mass transfer in the liquid boundary layer. Several expressions have been proposed over the years by various researchers on different membrane modules/configurations, which are compiled in Table 1. Many of them were developed based on fitting a general Sherwood correlation expression with experimental data. The general Sherwood expression is expressed as follows:

$$k_{bl} = \frac{D}{d_h} a_1 \text{Re}^{a_2} \text{Sc}^{a_3} \left(\frac{d_h}{L}\right)^{a_4} \quad (26)$$

where a_1 , a_2 , a_3 , and a_4 are constants. Correlations obtained from fitting experimental data to Equation (26) may not always be applicable to a full-scale pervaporation unit as the “entrance region” effect (developing flow-velocity profile), which is relatively minor for a full-scale module, but becomes important for a bench-scale pervaporation. Compounding this problem are the difficulties of modeling mass transfer within the membrane, which is described in the paper authored by Lipnizki and Trägårdh (2001), and of experimentally measuring solute concentration distribution in the liquid boundary layer. One has to rely on overall mass transfer data to infer the mass transfer in the boundary layer. As a result, prediction of VOC flux with one of these correlations in a full-scale unit evaluation could lead to overestimation of the concentration polarization effect. Some researchers employed “dead-end” types of pervaporation cells with magnetic stirrers to verify the membrane mass transfer models. However, the common assumption that stirring inside the “dead-end” membrane cell eliminates concentration polarization is not convincing. Furthermore, the overall mass transfer picture of a “dead-end” cell is not the same as a membrane cell with cross-flow mode, even through the operating conditions (membrane material/area, temperature, vacuum, and feed concentration) are the same. Thus, use of the model of mass transfer inside a membrane obtained from a “dead-end” experiment to infer the mass transfer in the boundary layer of a membrane cell with cross-flow mode is not compelling.

In order to effectively facilitate VOC removal, the permeation flux of VOCs during pervaporation operations should be maximized. In practical operations, concentration polarization can be reduced by

increasing the feed flow rate, using a pervaporation module configuration that is less susceptible to concentration polarization. For example, use of spiral wounded modules with turbulence-inducing spacers may help increase VOC removal in some circumstances. Obviously, advantages and disadvantages of this particular type of module should be evaluated before any operational decision is made. Overall, λ and CPI are interlinked parameters; the adjustment of one leads to the change of the other. Optimal operating conditions for VOC removal should be obtained by considering the specific objective of the operation, properties of the feedstock, and economy. The model proposed here can help provide the initial assessment of efficacy of a pervaporation process for this recovery purpose.

CONCLUSION

This paper introduces a new modeling approach to describing boundary-layer mass transport that has been the center of attention lately in membrane research because of the importance of concentration polarization on overall process performance, and lack of suitable modeling tools at hand. The model presented in this paper is able to establish the link between concentration polarization (via CPI) and mass transport in both longitudinal and transmembrane directions. Simulation results demonstrated in the plots correspond to conclusions of sensitivity analyses of operating parameters in experimental observations for a membrane module with similar configuration as described here (Wijmans et al., 1996). We envision the model can be incorporated into an integrated VOC removal system model that will provide simulation services to practitioners and system integrators. Designers of membrane modules and membrane materials should also find it useful in early stages of developmental work.

ACKNOWLEDGEMENTS

The research leading to this paper was supported jointly by the U.S. Environmental Protection Agency and New Jersey Agriculture Experiment Station at Rutgers University. This paper has not been subjected to the agency's peer and administrative review, and therefore may not necessarily reflect the reviews of the agency, and no official endorsement should be inferred.

NOMENCLATURE

- | | |
|---|--|
| A | cross-section area of the membrane channel, m ² |
| c | concentration of solute, kg/m ³ |

CPI	concentration polarization index, dimensionless
d_h	hydraulic diameter, m
D	diffusivity, m^2/s
h	half-height of the channel, m
k	mass transfer coefficient, m/s
L	length of the channel, m
M	mass flow rate, kg/m^3hr
u	flow velocity in the horizontal direction (x-axis), m/s
U	uniform or average bulk velocity in x direction, m/s
W	width of the channel, m
x	horizontal axis, m
y	vertical axis, m
Y	yield, dimensionless

Greek Letters

η	coordinate in y direction, dimensionless
θ	coordinate in y direction, dimensionless
λ	relative thickness of boundary layer in the channel, dimensionless
δ	boundary-layer thickness, m
ρ	density of fluid, kg/m^3
μ	viscosity

Superscripts and Subscripts

ov	overall
bl	boundary layer
m	membrane
diff	diffusion
b	border
long	longitudinal

0	zero
m	membrane
max	maximum
h	hydraulic
c	concentration

REFERENCES

- Abou-Nemeh, I., A. Das, A. Saraf, and K.K. Sirkar, 1999. A Composite Hollow Fiber Membrane-Based Pervaporation Process for Separation of VOCs from Aqueous Surfactant Solutions, *J. of Memb. Sci.*, 158, pp. 187-209.
- Aiouache, F., and S. Goto, 2003. Reactive Distillation–Pervaporation Hybrid Column for Tert-Amyl Alcohol Etherification with Ethanol, *Chem. Eng. Sci.*, 58, pp. 2465-2477.
- Alvarez, S., F.A. Riera, R. Alvarez, J. Coca, F.P. Cuperus, S.Th. Bouwer, G. Boswinkel, R.W. van Gemert, J.W. Veldsink, L. Giorno, L. Donato, S. Todisco, E. Drioli, J. Olsson, G. Trägårdh, S.N. Gaeta, and L. Panyor, 2000. A New Integrated Membrane Process for Producing Clarified Apple Juice and Apple Juice Aroma Concentrate, *J. Food Eng*, 46, pp.109-125.
- Bandini, S., A. Saavedra, and G.C. Sarti, 1997. Vacuum Membrane Distillation: Experiments and Modeling, *AIChE Journal*, 43(2), pp. 398-408.
- Berman, A.S., 1953. Laminar Flow in Channels with Porous Walls, *J. of Appl. Phy.*, 24, pp. 1232-1235.
- Bhattacharya, S., and S.-T. Hwang, 1997. Concentration Polarization, Separation Factor, and Peclet Number in Membrane Processes. *J. of Memb. Sci.*, 132, pp. 73-90.
- Binning, R. C., R. J. Lee, J.F. Jennings, and E. C. Martin, 1961. Separation of Liquid Mixtures by Permeation. *Ind. Eng. & Chem.*, 53, pp. 45-50.
- Bird, R. B., W. E. Steward, and E. N. Lightfoot, 2001. *Transport Phenomena* (2nd ed.). Wiley, New York, p. 625.
- Böddeker, K. W., G. Bengtson, and E. Bode, 1990a. Pervaporation of Low Volatility Aromatics from Water, *J. of Memb. Sci.*, 53, pp. 143-158.
- Böddeker, K. W., G. Bengtson, and H. Pingel, 1990b. Pervaporation of Isomeric Butanols, *J. of Memb. Sci.*, 54, pp. 1-12.
- Côté, P., and C. Lipski, 1988. Mass Transfer in Pervaporation for Water and Wastewater Treatment. In: R. A. Bakish (ed.), *Proceedings of 3rd International Conference on Pervaporation Processes and Chemical Industry*, pp. 449-462.

- Cussler, E. L., 1997. *Diffusion Mass Transfer in Fluid Systems*. Cambridge University Press, Cambridge, England, 2nd ed, p. 343.
- Dotremont, C., S. Van den Ende, H. Vandommele, and C. Vandecasteele, 1994. Concentration Polarization and Other Boundary-Layer Effects in the Pervaporation of Chlorinated Hydrocarbons, *Desalination*, 95, pp. 91-113
- George, S.C., K.N. Ninan, and S. Thomas, 2000. Pervaporation Separation of Chlorinated Hydrocarbon and Acetone Mixtures with Crosslinked Styrene-Butadiene Rubber and Natural Rubber Blend Membranes, *J. of Memb. Sci.*, 176, pp.131-142.
- Higuchi, A., B.-O. Yoon, T. Asano, K. Nakaegawa, S. Miki, M. Hara, Z. He, and I. Pinnau, 2002. Separation of Endocrine Disruptors from Aqueous Solutions by Pervaporation, *J. of Memb. Sci.*, 198, pp. 311-320.
- Hilmioğlu, D. N., and S. Tulbentci, 2003. Separation of IPA/Water Mixtures by Pervaporation: Sorption and Pervaporation Results, *Vacuum*, 72, pp. 35-40.
- Jiang, J.-S., L. M. Vane, and S. K. Sikdar, 1997a. Recovery of VOCs from Surfactant Solutions by Pervaporation, *J. of Memb. Sci.*, 136, pp. 233-247.
- Jiang, J.-S., D.B. Greenberg, and J.R. Fried, 1997b. Pervaporation of Methanol from A Triglyme Solution Using A Nafion Membrane: 2. Concentration Polarization, *J. of Membr. Sci.*, 132, pp. 263-271.
- Jiratananon, R., A. Chanachai, and R. Y. M. Huang, 2002. Pervaporation Dehydration of Ethanol–Water Mixtures with Chitosan/Hydroxyethylcellulose (CS/HEC) Composite Membranes: II. Analysis of Mass Transport, *J. of Memb. Sci.*, 199, pp. 211-222.
- Karlsson, H.O.E., and G. Trägårdh, 1996. Applications of Pervaporation in Food Processing, *Trends Food Sci Technol.*, 7, pp. 78-83.
- Kusakabe, K., S. Yoneshige, and S. Morooka, 1998. Separation of Benzene/Cyclohexane Mixtures Using Polyurethane–Silica Hybrid Membranes, *J. of Memb. Sci.*, 149, pp. 29-37.
- Lee, K.-R., M.-Y. Teng, H.H. Lee, and J.-Y. Lai, 2000. Dehydration of Ethanol/Water Mixtures by Pervaporation with Composite Membranes of Polyacrylic Acid and Plasma-Treated Polycarbonate, *J. of Memb. Sci.*, 164, pp. 13-23.
- Lipski, C., and P. Côté, 1990. The Use of Pervaporation for the Removal of Organic Contaminants from Water, *Environmental Progress*, 9, pp. 254-261.
- Lipnizki, F., and G. Trägårdh, 2001. Modelling of Pervaporation: Models to Analyze and Predict the Mass Transport in Pervaporation. *Separ. & Purification Methods*, 30(1), pp. 49-125.

- Matsui, S., and D. R. Paul, 2003. Pervaporation Separation of Aromatic/Aliphatic Hydrocarbons by SeS-Series of Ionically Crosslinked Poly(N-Alkyl Acrylate) Membranes, *J. of Memb. Sci.*, 213, pp. 67-83.
- Michael, A. S., 1995. Effects of Feed-Side Solute Polarization on Pervaporative Stripping of Volatile Organic Solutes from Dilute Aqueous Solution: A Generalized Analytical Treatment, *J. of Memb. Sci.*, 101, pp. 117-126.
- Mulder, M., 1991. *Basic Principles of Membrane Technology*, Kluwer Academic Publishers, Dordrecht, Netherlands, p. 286.
- Peng, M., L.M. Vane, and S.X. Liu, 2003. Recent Advances in VOCs Removal from Water by Pervaporation, *J. of Haz. Mat.*, B98, pp. 69-90.
- Peng, M., and S.X. Liu, 2003a. Recovery of Aroma Compounds from Dilute Model Blueberry Solution by Pervaporation, *J. Food Sci.*, 68, pp. 2706-2710.
- Peng, M., and S.X. Liu, 2003b. VOC Removal from Contaminated Groundwater through Membrane Pervaporation. Part II: 1,1,1-Trichloroethane-SDS Surfactant Solution System, *J. Environ. Sci.*, 15, pp. 821-826.
- Psaume, J., Ph. Aptel, Y. Aurelle, J.C. Mora, and J. L. Bersillon, 1986. Pervaporation: Importance of Concentration Polarization in the Extraction of Trace Organics from Water, *J. of Memb. Sci.*, 36, pp. 373-384.
- Rautenbach, R., and U. Hommerich, 1998. Experimental Study of Dynamic Mass Transfer Effects in Pervaporation, *AIChE Journal*, 44, pp.1210-1215.
- Schlichting, H., 1979. *Boundary Layer Theory*, McGraw-Hill, New York, 7th ed., P. 158.
- Shepherd, A., A.C. Habert, and C.P. Borges, 2002. Hollow Fibre Modules for Orange Juice Aroma Recovery Using Pervaporation, *Desalination*, 148, pp. 111-114.
- Shieh, J.-J., and R. Y. M. Huang, 1998. Chitosan/N-methylol Nylon 6 Blend Membranes for the Pervaporation Separation of Ethanol–Water Mixtures, 148, pp. 243-255.
- Urriaga, A.M., E.D. Gorri, J.K. Beasley, and I. Dritz, 1999. Mass Transfer Analysis of the Pervaporative Separation of Chloroform from Aqueous Solutions in Hollow Fiber Devices, *J. Membr. Sci.*, 156, pp. 275-291.
- Uragami, T., H. Yamada, and T. Miyata, 2001. Removal of Dilute Volatile Organic Compounds Water Through Graft Copolymer Membranes Consisting of Poly(Alkylmethacrylate) and Poly(Dimethylsiloxane) by Pervaporation and Their Membrane Morphology, *J. of Memb. Sci.*, 187, pp. 255-269.

- Vane, L. M., F. R. Alvarez, and E. L. Giroux, 1999. Reduction of Concentration Polarization in Pervaporation Using Vibrating Membrane Module, *J. of Memb. Sci.*, 153, pp. 233-241.
- Vane, L. M., and F.R. Alvarez, 2002. Full-Scale Vibrating Pervaporation Membrane Unit: VOC Removal from Water and Surfactant Solutions, *J. of Memb. Sci.*, 202, pp. 177-193.
- Wijmans, J. G., A. L. Athayde, R. Daniels, J. H. Ly, H. D. Kamaruddin, and I. Pinnau, 1996. The Role of Boundary Layers in the Removal of Volatile Organic Compounds from Water by Pervaporation, *J. of Memb. Sci.*, 109, pp. 135-146.

Original Manuscript Recieved: June 17, 2003

Revised Manuscript Recieved: December 1, 2003